

Stepped chirped fiber Bragg grating encoder/decoder for spectral OCDMA

Xiaohui Fang (方晓惠)¹, Shichen Li (李世忱)¹, Hebin Tian (田贺斌)¹, and Dongning Wang (王东宁)²

¹College of Precision Instrument and Opto-Electronics Engineering, Tianjin University, Tianjin 300072

²Department of Electrical Engineering, Hongkong Polytechnic University, Hongkong

Received November 28, 2002

Based on the coupled-mode theory of fiber grating and codes theory, the design of an optical code division multiple access (OCDMA) encoder/decoder with stepped chirped fiber Bragg grating (SCFBG) has been proposed. The length of each uniform subgrating, the realization of encoding and decoding are provided. Numerical result is also presented and discussed.

OCIS codes: 050.2770, 060.2330, 060.2340.

OCDMA technique recently has attracted considerable attention as a potential candidate for multiplexing of high speed fiber optical local area networks (LANs).

Encoder/decoder is the key component in OCDMA technique. In the earliest implementation, optical fiber delay line (OFDL) encoder/decoder, which operates code in time domain, has defect of inexact delay and poor reproduction in fabrication^[1]; traditional 4F grating-pair device encoder/decoder, which operates in frequency domain, is hindered in fiber optical communication for its physical and coupling efficiency limitation^[2,3]. Encoder/decoder based on fiber grating has attracted much attention due to its good reproduction in fabrication and easy coupling with optical fiber communication system. Moreover, stringent requirements of DWDM technique boost improvement and enhancement of fiber grating fabrication technique: from common uniform fiber grating to all kinds of chirped grating, now it is possible to design and reliably fabricate superstructured fiber Bragg gratings (FBGs)^[4,5] with truly complex amplitude and phase responses. The progress of the fabrication of FBG makes it possible to realize phase encoding and decoding in FBG^[6-9].

Use of phase coding is significant since it is well known that bipolar codes exhibit better cross-correlation crosstalk characteristics than unipolar codes. This key aspect of phase encoding allows lower interchannel interference and thus more simultaneous users for a given code length than unipolar coding. This ultimately permits a higher overall system spectral efficiency than unipolar coding.

In Ref. [7], a phase coding OCDMA system was demonstrated, but no code and detail theory analyses are given. This paper will discuss the design of the encoder, decoder and realization of system in detail.

Figure 1 is the schematic of encoder/decoder based on a pair of SCFBGs. The device includes a pair of SCFBGs arranged in series. By SCFBGs, it means gratings composed of spatially adjacent subgratings, each of which has constant spatial period but between of which has constantly incremented one. When an input bit is incident on the SCFBG1, the wavelengths are dispersed in time and the reflected pulse is temporally expanded. When this expanded bit reflected from a SCFBG has an opposite dispersion slope, the wavelength components are

resynchronized and the original pulse is reconstituted. However if the SCFBG2 contains phase-shift along its length, these phase-shifts are transferred to the reflected signal and the output pulse represents a spectral-phase-encoded bit. The encoder data bit transmitted through network until it reached a receiver. For data bit encoded, only those whose address code matches that in the decoder can be decoded by auto-correlation detection, otherwise there is multi-access interference at the output of decoder.

Bandwidth from peak to the first zero of reflection spectrum in uniform period grating is given by

$$\delta\lambda = \frac{\lambda^2}{2\pi n_{\text{eff}}\delta l} \sqrt{(\kappa\delta l)^2 + \pi^2}, \quad (1)$$

where κ is coupling index, n_{eff} is effective refractive index in fiber grating, and δl is the length of each subgrating. Considering weak coupling condition $\kappa\delta l \ll \pi^2$, thus

$$\delta\lambda = \frac{\lambda^2}{2n_{\text{eff}}\delta l}. \quad (2)$$

Total length l of fiber grating equals to the sum of each length of subgrating δl . To ensure that each subgrating controls the backward diffraction of an isolated spectral band, we design the length of each subgrating to satisfy the relationship that $\delta\lambda$ equals to the increase of Bragg wavelength of neighbor subgrating, that is $\delta\lambda = \lambda_{Bn} - \lambda_{Bn-1} = \delta\lambda_{\text{chirp}}$.

Using the matrix analysis method, the relationship between initial point ($l = 0$) and the end of the grating ($l = L$) for forward/backward transmission wave amplitudes can be expressed by

$$\begin{bmatrix} A(L) \\ B(L) \end{bmatrix} = T \begin{bmatrix} A(0) \\ B(0) \end{bmatrix}. \quad (3)$$

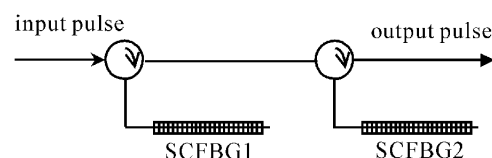


Fig. 1. Schematic of encoder/decoder based on a pair of SCFBGs.

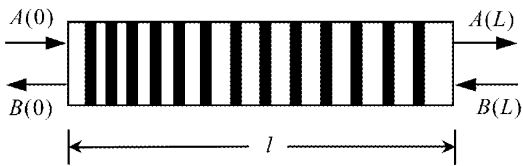


Fig. 2. Amplitude transaction and reflection of step chirped FBG.

The T matrix in Eq. (3) is the product of scattering matrix of N grating in series, which is given by

$$T(0, L) = T_N(z_{N-1}, z_N) \cdots T_2(z_1, z_2) \cdot T_1(z_0, z_1), \quad (4)$$

where $z_0 = 0$, $z_N = L$, and $T_n(z_{n-1}, z_n)$ represents matrix of each subgrating^[10]

$$T_n(z_{n-1}, z_n) = \begin{bmatrix} e^{-i\delta\beta_n(z_n - z_{n-1})/2} p_n & e^{-i\delta\beta_n(z_n + z_{n-1})/2} q_n \\ e^{i\delta\beta_n(z_n + z_{n-1})/2} q_n^* & e^{i\delta\beta_n(z_n - z_{n-1})/2} p_n^* \end{bmatrix}, \quad (5)$$

$$p_n(z_n - z_{n-1}) = \left\{ \cosh[\alpha_n(z_n - z_{n-1})] + i \frac{\delta\beta_n}{\alpha_n} \sinh[\alpha_n(z_n - z_{n-1})] \right\}, \quad (6)$$

$$q_n(z_n - z_{n-1}) = i \frac{\kappa_n}{\alpha_n} \sinh[\alpha_n(z_n - z_{n-1})], \quad (7)$$

where p_n^* and q_n^* are the complex conjugates of p_n and q_n respectively, $\delta\beta_n = 2\pi(\lambda^{-1} - \lambda_{Bn}^{-1})$ is the detuning from the Bragg wavelength of the n th subgrating λ_{Bn} , and $\alpha_n = \sqrt{|\kappa_n|^2 - (\delta\beta_n)^2}$. Considering boundary condition $B(L) = 0$, the amplitude reflection coefficient at point of $l = 0$ can then show to be

$$r = \frac{B(0)}{A(0)} = -\frac{T_{21}}{T_{22}}. \quad (8)$$

Assign an address code to the k th user $c^k = (c_0^k, c_1^k, \dots, c_{N-1}^k)$, where $c_n^k \in \{1, -1\}$. Using maximum-sequence as address code is well known as one of PN sequence and its correlation property is also known. We consider each subgrating as an encoding unit, adding phase shift $\phi_n^k \in (0, \pi)$, which corresponding to $c_n^k \in \{1, -1\}$ in the unit. When $\phi_n^k = \pi$, the phase-shift matrix is^[10]

$$\phi = \begin{bmatrix} e^{-i\pi/2} & 0 \\ 0 & e^{i\pi/2} \end{bmatrix}. \quad (9)$$

When $\phi_n^k = 0$, the phase shift matrix is a unit matrix. For example, using a maximum sequence with code length 7 (1, 1, -1, -1, 1, -1, 1) as an address code, inserting corresponding phase shift into the SCFBG during fabrication, then Eq. (4) is changed by

$$T = T_7 \cdot \phi \cdot T_6 \cdot T_5 \cdot \phi \cdot T_4 \cdot \phi \cdot T_3 \cdot T_2 \cdot T_1. \quad (10)$$

Unit matrix is omitted in Eq. (10), because for a decoder matched with the encoder, its structure is the same as that in the encoder except that the corresponding

phase shift matrix is conjugate with the one in encoder.

If the power spectrum of the input pulse is a constant over the entire spectral bandwidth, by inverse Fourier transform, the time domain expression of the optical pulse passed through SCFBG1 and SCFBG2 in the encoder can be written respectively as

$$C_{1k}(t) = i \tanh(\kappa\Delta z) \frac{\sqrt{P_0}}{N} \sum_{n=1}^N \sin c[\pi\Delta f(t + 2t_{n-1})] \times \exp(i2\pi f_{Bn}t), \quad (11)$$

$$C_{2k}(t) \approx -\frac{\sqrt{P_0}}{N} \tanh^2(\kappa\Delta z) \sin c[\pi\Delta f(t + 2t_{N-1})] \times \sum_{n=1}^N \exp(i2\pi n f_{Bn}t) \cdot \exp(i\phi_n^k) = \frac{\sqrt{P_0}}{N} \tanh^2(z) \sin c[\pi\Delta f(t + 2t_{N-1})] \times \sum_{n=1}^N c_n^k \exp(i2\pi f_{Bn}t), \quad (12)$$

where P_0 is the total power of the input pulse, $f_n = c/\lambda_n$, $\Delta f = \frac{c\Delta\lambda}{\lambda_0^2}$ (λ_0 is central wavelength of SCFBG), $t_{n-1} = \frac{n_{\text{eff}} z_{n-1}}{c}$ is the time delay associated with each spectral band, representing dispersion property of the chirped fiber grating. After the signal pulse passed through SCFBG2, which exhibits opposite dispersion slope with SCFBG1, the dispersion obtained from SCFBG1 can be compensated by SCFBG2, in other words, the same time delay $2t_{N-1}$ can be obtained for all the spectral segments. Thus if no phase shift exists between any pair of subgratings of SCFBG2, pulse will be reconstructed; otherwise the pulse of SCFBG2 represents a spectral phase encoded bit.

In decoding process, only data bit whose address code matches that in decoder can be decoded by auto-correlation detection, otherwise there is multi-access interference at the output of the decoder. The electric field representation of k th decoder output can be written as

$$r_m(t) = C_{kk}(t) + \sum_{k \neq \nu} C_{\nu k}(t), \quad (13)$$

where $C_{kk}(t)$ is auto-correlation term, while $\sum_{k \neq \nu} C_{\nu k}(t)$ is cross-correlation term.

We assume that 1-ps Gaussian pulse is input into the encoder in the numerical calculation. Figure 3(a) is the reflection spectrum of a 15 step chirped FBG. The parameter used here is $n_{\text{eff}} = 1.456$, $\Delta n = 2.1 \times 10^{-4}$, and Bragg center wavelength increment is 0.3 nm from 1540.3 to 1545.0 nm in the SCFBG. Each reflection spectral band corresponding to each subgrating is not perfect isolated (ideally, it is flat), and in fact there exists overlap between neighbor spectral band. The overlap is determined by the length of each subgrating, and makes each Bragg center wavelength not at the peak of reflection spectrum. On the other hand, the side-lobe structure of

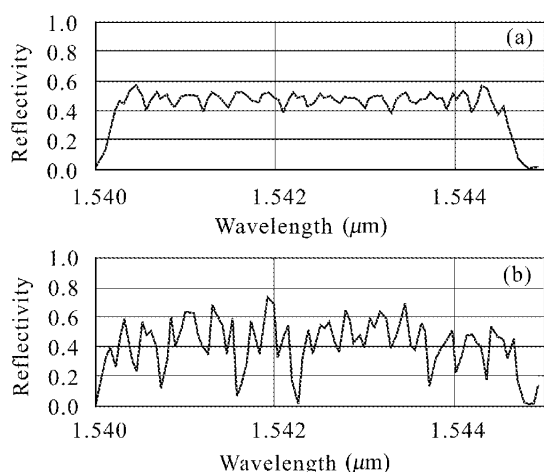


Fig. 3. Reflection spectrum of a stepped chirped FBG. (a) Reflectivity with no code; (b) reflectivity with code.

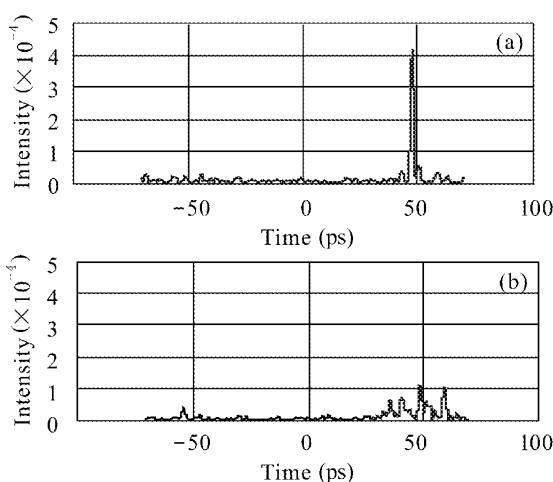


Fig. 4. Correlation curve based on pair of step chirped FBGs decoder with m sequence of code length 15. (a) Auto-correlation curve; (b) cross-correlation curve.

reflection spectrum in each subgrating will also influence the total spectrum and correlation property. Figure 3(b) is the reflection spectrum of the SCFBG inserted phase shifts in serial as address code. The parameter used here is the same as that used in the Fig. 3(a). We choose a maximum sequence with code length 15 $(-1, -1, -1, 1, 1, 1, -1, 1, -1, 1, 1, -1, -1, 1)$ as address code, inserting corresponding phase shifts into each subgrating.

Figure 4 is the intensity correlation after coded data bit passing through the decoder based on SCFBGs. Figure 4(a) is auto-correlation curve, 4(b) is cross-correlation curve. When address code in the decoder matches with

that in data bit, auto-correlation is obtained. Otherwise, cross-correlation will be obtained which become multi-access interference in signal detection. From Fig. 4, we also see that the peak of auto-correlation is not at zero point of time axis. This is because we choose $t = 0$ when initial pulse peak is input into the encoder. Although the wavelength components are resynchronized at the output of decoder, they experience a time delay from two pairs of SCFBGs (encoder and decoder). This is just the result of Eq. (13). The performance of cross-correlation is not only determined by maximum sequence itself which is not an orthogonal sequence, but also related to the side-lobe structure of reflection spectrum of each subgrating. And when side-lobes are large, the correlation property will become worse; the imperfect isolated reflection spectral band of each subgrating will also influence the performance of cross-correlation. Besides, the use of the longer code sequence provides much better auto-correlation contrast than that achieved with a shorter code sequence due to property of maximum sequence.

In summary, design of encoder/decoder based on SCFBGs is proposed in this paper. Encoder or decoder is made up of a pair of SCFBGs in which the second one is phase coded. The length of each subgrating and realization of encoding/decoding are provided. Numerical result shows that good performance of correlation is obtained.

This work was supported by the National Natural Science Foundation of China (69877012). X. Fang's e-mail address is fang_xiaohui@eyou.com.

References

1. M. E. Marhic, *J. Lightwave Technol.* **11**, 854 (1993).
2. M. M. Wefers and K. A. Nelson, *Opt. Lett.* **18**, 2032 (1993).
3. K. Kamakura, T. Ohtsuki, and I. Sasase, *IEICE Trans. Commun.* **E82-B**, 1038 (1999).
4. C.-Y. Lin, G.-W. Chern, and L. A. Wang, *J. Lightwave Technol.* **19**, 1212 (2001).
5. L. R. Chen, H. S. Loka, D. J. F. Copper, P. W. E. Smith, R. Tam, and X. Gu, *Electron. Lett.* **35**, 584 (1999).
6. P. C. Teh, P. Petropoulos, M. Ibsen, and D. J. Richardson, *IEEE Photon. Technol. Lett.* **13**, 154 (2001).
7. A. Grunnet-Jepsen, A. E. Johnson, E. S. Maniloff, T. W. Mossberg, M. J. Munroe, and J. N. Sweetser, *Electron. Lett.* **35**, 1096 (1999).
8. J.-F. Huang and D.-Z. Hsu, *IEEE Photon. Technol. Lett.* **12**, 1252 (2000).
9. L. R. Chen, S. D. Benjamin, P. W. E. Smith, J. E. Sipe, and S. Juma, *Opt. Lett.* **22**, 402 (1997).
10. M. McCall, *J. Lightwave Technol.* **18**, 236 (2000).